

Article

Not peer-reviewed version

Abscisic Acid Enhances Ex-Vitro Acclimatization Performance in Hop (*Humulus lupulus L.*)

[Luciana Di Sario](#) , [David Navarro-Payá](#) , [Fany Zubillaga](#) , [José Tomás Matus](#) , [Patricia Boeri](#) ^{*} ,
[Gastón Alfredo Pizzio](#) ^{*}

Posted Date: 30 May 2025

doi: 10.20944/preprints202505.2415.v1

Keywords: PYR/PYLs gene family; abiotic stress; ABA perception; in-vitro propagation; rustication



Preprints.org is a free multidisciplinary platform providing preprint service that is dedicated to making early versions of research outputs permanently available and citable. Preprints posted at Preprints.org appear in Web of Science, Crossref, Google Scholar, Scilit, Europe PMC.

Copyright: This open access article is published under a Creative Commons CC BY 4.0 license, which permit the free download, distribution, and reuse, provided that the author and preprint are cited in any reuse.

Disclaimer/Publisher's Note: The statements, opinions, and data contained in all publications are solely those of the individual author(s) and contributor(s) and not of MDPI and/or the editor(s). MDPI and/or the editor(s) disclaim responsibility for any injury to people or property resulting from any ideas, methods, instructions, or products referred to in the content.

Article

Abscisic Acid Enhances Ex-Vitro Acclimatization Performance in Hop (*Humulus lupulus L.*)

Luciana Di Sario ¹, David Navarro-Payá ², Fany Zubillaga ¹, José Tomás Matus ², Patricia Boeri ^{1,*} and Gastón A. Pizzio ^{1,2,*}

¹ Universidad Nacional de Río Negro, CIT-RIO NEGRO, Viedma CP8500, Río Negro, Argentina

² Institute for Integrative Systems Biology (I2SysBio), Universitat de València-CSIC, Paterna, 46908 Valencia, Spain

* Correspondence: gapizzio@gmail.com (G.A.P.); pboeri@unrn.edu.ar (P.B.)

Abstract: *Humulus lupulus L.* (hop) is a multipurpose crop valued for its essential role in beer production and for its bioactive compounds with recognized medicinal properties. Otherwise, climate change represents a major challenge to agriculture, particularly impacting the cultivation of crops with stenocious characteristics, such as *hop*. This highlights the urgent need to enhance crop resilience to adverse environmental conditions. The phytohormone abscisic acid (ABA) is a key regulator of plant responses to abiotic stress, yet the ABA signaling pathway remains poorly characterized in hop. Harnessing the publicly available hop genomics resources, we identified eight members of the PYRABACTIN RESISTANCE 1 LIKE ABA receptor family (HIPYLs). Phylogenetic and gene structure analyses classified these HIPYLs into the three canonical ABA receptor subfamilies. Furthermore, all eight HIPYLs are likely functional, suggested by the protein sequence visual analysis. Expression profiling indicates that ABA perception in hop is primarily mediated by the HIPYL1-like and HIPYL8-like subfamilies, while the HIPYL4-like group appears to play a more limited role. Structure modeling and topology predictions of HIPYL1b and HIPYL2 provided insights into their potential functional mechanisms. To assess the physiological relevance of ABA signaling in hop, we evaluated the impact of exogenous ABA application during the *ex-vitro* acclimatization phase. ABA-treated plants exhibited more robust growth, reduced stress symptoms and improved acclimatization success. These effects were associated with reduced leaf transpiration and enhanced stomatal closure, consistent with ABA-mediated drought tolerance mechanisms. Altogether, this study provides the first comprehensive characterization of ABA receptor components in hop and demonstrates the practical utility of ABA in improving plant performance under *ex-vitro* conditions. These findings lay the groundwork for further functional studies and highlight ABA signaling as a promising target for enhancing stress resilience in hop, with broader implications for sustainable agriculture in the face of climate change.

Keywords: PYR/PYLs gene family; abiotic stress; ABA perception; *in-vitro* propagation; rustication

1. Introduction

Humulus lupulus L. (hop) is a well-known crop in the brewing industry, valued for its contribution of key bittering and flavoring components such as bitter acids, flavonoids and essential oils. Beyond its industrial use, hop is also classified as a medicinal plant due to its rich array of bioactive compounds with significant therapeutic potential. Notably, it produces prenyl flavonoids, including xanthohumol (XN) and 8-prenylnaringenin (8-PN), which have been widely studied for their health-promoting properties [1].

Hop is a dioecious perennial plant that is productive for about 25 years. Adult plants reach a height of 7–10 m, growing up to 30 cm per day during the main vegetation period [2]. The hop tissue with commercial value is the inflorescence of female plants, which is called strobili or cone. In

contrast, the male plants that contain pollen-producer flowers (pollinator plants) are kept away from the cultivated areas to prevent the formation of seeds in the cones due to pollination, thus ensuring a genetically constant product [2]. However, male plants are essential for breeding programs [1]. Hop flowering is in summer: male inflorescences are panicle-shaped, while female inflorescences are ovoid and consist of a central rachis bearing small bracts at each node. During flowering, the rachis elongates, the size of the bracts increases, and a large amount of glandular trichomes develop in the lower part of the bracts, which contain a yellow resin called lupulin [1]. The number and size of glands depends mainly on genetic differences between cultivars [3]. The secondary metabolites present in the cones of hops are the main aroma compounds in beer. Lupulin accounts for 10–30% of the cone dry weight and the most important flavoring agent is the bitterness of alpha and beta acids, known collectively as bitter acids. Other important aroma compounds include prenylated flavonoids such as xanthohumol and volatile secondary metabolites or “hop oils” [4]. In addition, thiol precursors have recently attracted attention for their contribution to popular flavors [5–7].

Hop plants production by seeds or vegetative propagation (rhizomes and cuttings) may result in strong disadvantages, such as male plants propagules, poor phytosanitary quality and accumulations of pathogens that reduce productivity [8]. *In-vitro* propagation of hops represents an effective alternative [9,10]. For instance, *in-vitro* plant regeneration from meristems produces high phytosanitary quality propagules, which prevents and control pathogens dissemination in hop cultivation. Additionally, *in-vitro* propagation of nodal segments ensures female plant production with low genetic variability. Nevertheless, the efficiency of the acclimatization phase, during which plants adapt to *ex-vitro* conditions, plays a critical role in the success of micropropagation protocols. During this process, it is crucial to carefully address stomatal dysfunctions, high transpiration rates, and the presence of a thin cuticle, which can lead to plant wilting and senescence [11–13]. Several studies have linked these issues to the limited capacity of plants to produce abscisic acid (ABA) [14,15]. The phytohormone ABA plays a key role in inducing drought tolerance, among others abiotic stresses, and participates in different plant physiological processes, including stomatal closure, induction of antioxidant capacity and synthesis of osmoprotectant solutes [16–18]. On the other hand, high temperatures and low water irrigation during the growing season have been shown to reduce hop cone yield and cone bitterness [19–22]. Additionally, it was reported a positive correlation between hop yield and irrigation, as well as a negative correlation between summer high temperature and alpha acid content [22]. These results agree with previous reports that found lower hop yield in years with low rainfall, and lower alpha acid content in years with high temperatures [19,20].

ABA is involved in several physiological processes, such as seed and bud dormancy [23,24], organ development [25], and fruit maturation [26,27], among others. For instance, ABA triggers stomatal closure [18,28], regulates the hydraulic response to prolonged drought [29], controls carbohydrate metabolism during recovery from stress [30], and modulates salt perception and posterior exclusion when plants are under salinity stress [31,32]. Additionally, ABA regulates the secondary metabolism to enhance plant acclimatization to abiotic stress, for instance by increasing the content of different terpenes and anthocyanins with antioxidant properties [33,34]. Moreover, ABA also induces the production of osmocompatible solutes, such as proline, betaines, galactinol, and sugars [35–38].

ABA is a sesquiterpenoid phytohormone derived from carotenoids. The first steps (cleavage of 9-cis-violaxanthin or 9'-cis-neoxanthin by NCED enzymes) occur in plastids. The resulting product (xanthoxin) is then exported to the cytosol, where it is converted into ABA [39]. ABA is mainly produced by the root system and transported from the roots to the leaves via the transpiration current along the xylem [40,41]. However, drought-induced ABA production is also present in leaf mesophyll cells [42,43]. The ABA signal transduction pathway is then initiated by the hormone perception in target cells by the family of PYRABACTIN RESISTANCE1 LIKE (PYL) receptors [17,44]. ABA perception induces the formation of a ternary complex between ABA, PYL receptors, and clade A protein phosphatase type 2C (PP2Cs) [45–47]. Consequently, inhibition of the subclass III SNF1-related protein kinases 2 (SnRK2s) by PP2Cs is abolished [48,49]. ABA-activated SnRK2s turn-on the

down-stream signaling through different effectors, from transmembrane channels to transcription factors [17]. In a second level of regulation, the activity and half-life of the core ABA signaling components are regulated by accessory kinases, the proteasome system pathway and the circadian system [50–53].

Climate change brings significant challenges to agriculture and food production impacting crops that thrive in regions with specific environmental requirements, i.e., those with stenocious characteristics, such as *Humulus lupulus L.* Therefore, it is imperative to examine the ability of plants to withstand challenging environmental conditions. Plant response to abiotic stress heavily relies on ABA signal transduction, while the ABA receptor family has been methodically identified in a wide range of crops, such as quinoa [54,55], tomato [56], grape [57,58], wheat [59], rice [60], canola [61], palm [62] and benthamiana [63], among other species. To discover innovative strategies to cope with environmental stress and hop production this study aims to unravel the gene family of PYL receptors in *Humulus lupulus L.* and evaluate the role of ABA in leaf transpiration and ex-vitro acclimatization performance. Taking advantage of the public hop genomics resource [64,65] we have identified eight members of HIPYL ABA receptors, implementing the genome-search method. To categorize this HIPYL phylogenetic and gene structure analyses were conducted. The result grouped HIPYLs in the three classical subfamilies of ABA receptors: PYL1-like, PYL4-like and PYL8-like. Moreover, the expression pattern of *HIPYLs* at the tissue-specific level showed that PYL1-like and PYL8-like receptors are predominantly and should lead ABA perception across hop plants. By contrast, PYL4-like receptors should have residual functions. Additionally, to evaluate the potential of each *HIPYLs* to be functional, conserved domains analyses and visual examinations of protein sequence alignment were performed. In addition, the protein structure of *HIPYL1b* and *2* was modeled by homology and topology analysis was performed to visualize relevant distinctive residues. Finally, we have evaluated the role of ABA in regulating stomatal closure, leaf transpiration and plant *ex-vitro* acclimatization. As a result, both water loss and stress symptoms in plants were reduced, leading to improved growth performance.

2. Results

2.1. Genome-Wide Identification of PYLs in *H. lupulus*

The hop genome is approximately 2.8 Gb in size, distributed across 10 chromosomes ($2n = 18 + XY$) [64,65]. A total of eight *PYL* genes were identified in the hop genome (Table 1). The open reading frame (ORF) lengths of the *HIPYL* genes ranged from 558 bp to 669 bp, with an average of 582 bp, while the encoded proteins varied in length from 185 to 222 amino acids, averaging 193 residues. Chromosomal mapping revealed that these eight *HIPYL* genes are unevenly distributed across only three out of ten hop chromosomes (Figure 1). Notably, *HIPYL2* is located on the sexual chromosome 3. Besides, chromosome 5 harbours the highest number of *PYL* genes containing four *HIPYLs*, while chromosome 9 contains three. In contrast, chromosomes 1, 2, 4, 6, 7, and 10 contain no *HIPYL* genes (Figure 1).

Table 1. Basic information of ABA receptors in *Humulus lupulus L.*

Gene ID	Gene name	Genome location (start..stop)	ORF length (bp)	Protein size (aa)
HUMLU_CAS0037465	HIPYL1a	CH5/Scaffold 24 (101098846..101099927)	600	200
HUMLU_CAS0037437	HIPYL1b	CH5/Scaffold 24 (97872371..97873468)	603	201
HUMLU_CAS0026810	HIPYL2	CH3/Scaffold 1533 (420945668..420946409)	615	204
HUMLU_CAS0067482	HIPYL4a	CH9/Scaffold 49 (153780561..153781466)	579	192
HUMLU_CAS0067343	HIPYL4b	CH9/Scaffold 49 (147637069..147638078)	633	211
HUMLU_CAS0039633	HIPYL8a	CH5/Scaffold 24 (335968664..335971620)	579	192
HUMLU_CAS0039258	HIPYL8b	CH5/Scaffold 24 (323689689..323692723)	579	192
HUMLU_CAS0065351	HIPYL9	CH9/Scaffold 49 (93847944..93850402)	558	185

These eight unique proteins were identified and considered as candidate hop PYL proteins.

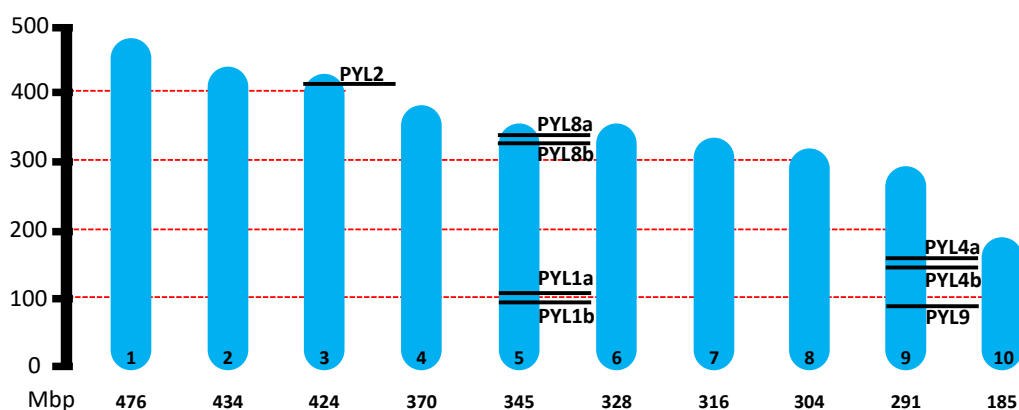


Figure 1. Chromosomal location of eight HIPYL genes across the *Humulus lupulus* genome. The ten chromosome (numbered inside) of hop are shown in scale based on their physical size. Under each chromosome the estimated size in Mbp: Mega base pair.

2.2. Phylogeny, Gene Structure Analysis and Tissue-Specific Expression Pattern of HIPYLs

To investigate the phylogenetic relationships of PYL receptors in *Humulus lupulus* L., a maximum-likelihood (ML) tree was constructed using full-length protein sequence alignments of the eight identified HIPYLs and 14 AtPYLs (Figure 2). As there is no standard nomenclature for PYL genes in hop, the HIPYLs were named based on their phylogenetic relationships with their *Arabidopsis thaliana* counterparts. Consistent with the previous studies in *Arabidopsis* and other species [17,44,54,58,66], HIPYLs clustered into three conserved subfamilies. Specifically, subfamily I included three gene members (*HIPYL8a*, *HIPYL8b*, and *HIPYL9*), subfamily II comprised two members (*HIPYL4a* and *HIPYL4b*), and subfamily III consisted of the remaining three genes (*HIPYL1a*, *HIPYL1b*, and *HIPYL2*).

To further support the phylogenetic classification, we analyzed the gene structure of HIPYLs, including untranslated regions (UTRs), exons, and introns, which can provide insights into gene family evolution [67] (Supplemental Figure S1). The analysis revealed that five genes were intronless (*HIPYL1a*, *HIPYL1b*, *HIPYL2*, *HIPYL4a* and *HIPYL4b*); whereas three genes (*HIPYL8a*, *HIPYL8b* and *HIPYL9*) contain two introns. Notably, genes within the same subfamily shared similar exon-intron structures, further validating the subfamily classifications derived from the phylogenetic analysis (Figure 2). To assess the tissue specific expression patterns of HIPYLs, we analyzed publicly available RNA-seq data across different tissues (adult leaf, shoot, root, and flower cones) and developmental stages (sprout, young plant, vegetative, and flowering) (Figure 3). The results revealed distinct expression profiles among HIPYL family members. Members of subfamily I (*HIPYL8b* and *HIPYL9*) and subfamily III (*HIPYL1a* and *HIPYL1b*) were highly expressed across most tissues and stages, suggesting they play a ubiquitous role in ABA perception and signaling. In contrast, subfamily II members (*HIPYL4a* and *HIPYL4b*) exhibited low or residual expression, indicating a potentially limited functional role under the conditions analyzed.

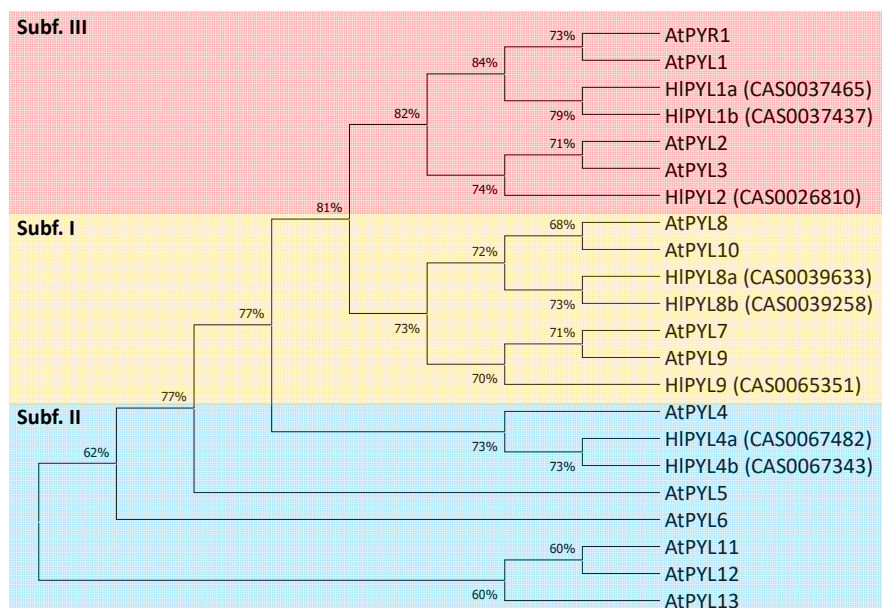


Figure 2. Phylogenetic analysis of PYL gene family in *Humulus lupulus L.* and *Arabidopsis thaliana*. Tree was built in MEGAx, using LG model and maximum-likelihood method (1000 bootstraps). Orange, blue and red clades represent subfamilies I, II and III, respectively. The percentage of replicate trees in which the associated taxa clustered together are shown next to the branches.

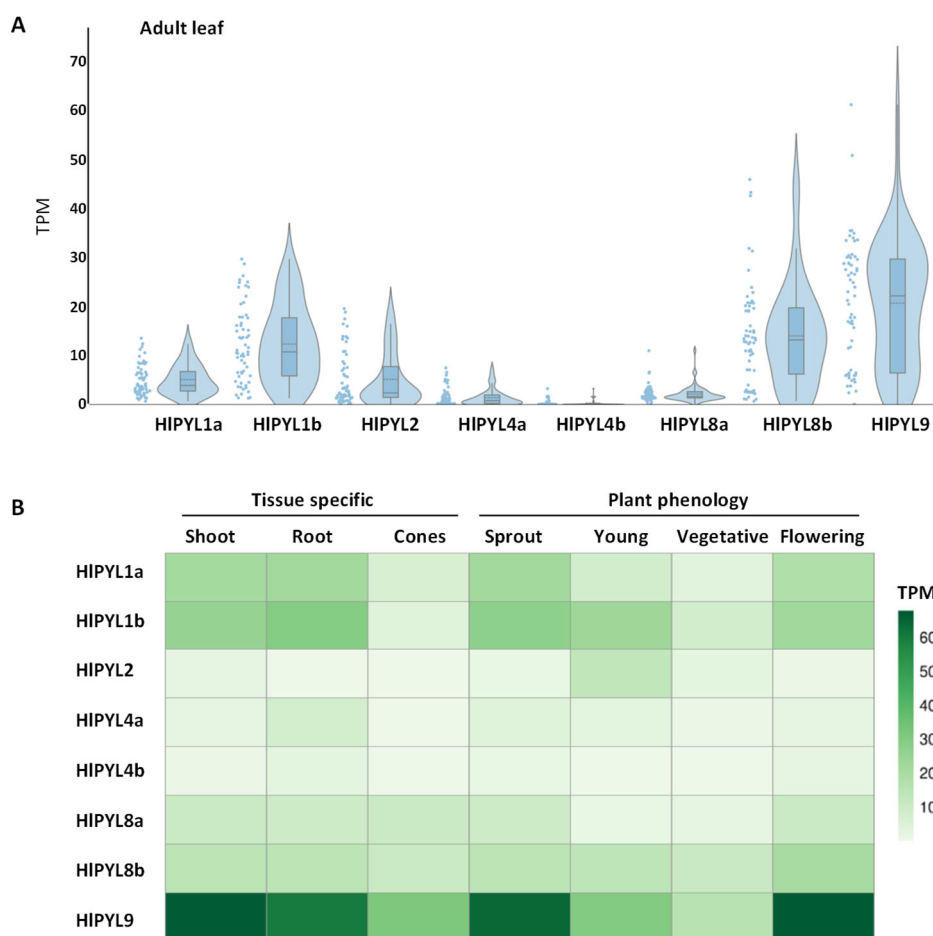


Figure 3. Tissue specific expression patterns of HIPYLs. (A) Leaf expression of hop PYL genes across public transcriptomic data. RNA-Seq raw data (Illumina; 61 runs) were downloaded from the SRA-NCBI and analyzed. Expression data was normalized to transcripts per kilobase of exon model per million mapped reads (TPM)

values. Violin plots show the overall frequency distribution of data points, while the inner boxplots mark interquartile ranges, mean (dotted line), and median (solid line) values. (B) Mean TPM is visualized in a heatmap of plant phenology and tissue specific *HIPYLs* expression. Public RNAseq corresponding leaf (Illumina; 61 runs), shoot system (Illumina; 25 runs), root (Illumina; 19 runs), cones (Illumina; 2 runs), sprout (Illumina; 44 runs), young plant (Illumina; 14 runs), vegetative (Illumina; 37 runs) and flowering (Illumina; 25 runs) were treated as in (A).

2.3. Conserved Motif, Protein Alignments and 3D Topology Analysis of PYLs in Hop

To confirm the presence of the PYR_PYL_RCAR domain in each *HIPYL* protein sequence, a motif/domain search was performed using the Pfam and NCBI-CDD databases via the MOTIF search tool. The PYR_PYL_RCAR domain is a hallmark of ABA receptors and is essential for their proper functionality. All eight *HIPYL* proteins identified in this study exhibited the presence of this conserved domain (Supplemental Figure S2), suggesting that they are likely functional ABA receptors.

A close inspection of the amino acid sequence and secondary structure alignment of the AtPYLs and *HIPYLs*, generated using ESPRIPT [68], shows a high degree of conservation (Figure 4). Is particularly relevant, the conservation of key features involved in ABA binding such as the gate loop and the latch loop [69]. Besides, it is also observed a conservation in key residues required for hormone-receptor interaction (Figure 4). This fact is in agreement with the idea that the eight *HIPYLs* are functional, capable to bind ABA and to form the ternary complex with PP2Cs proteins. It is interesting to note that *HIPYL2* has a novel extra loop, between B6-B7 sheets, close to the latch loop (Figure 4).

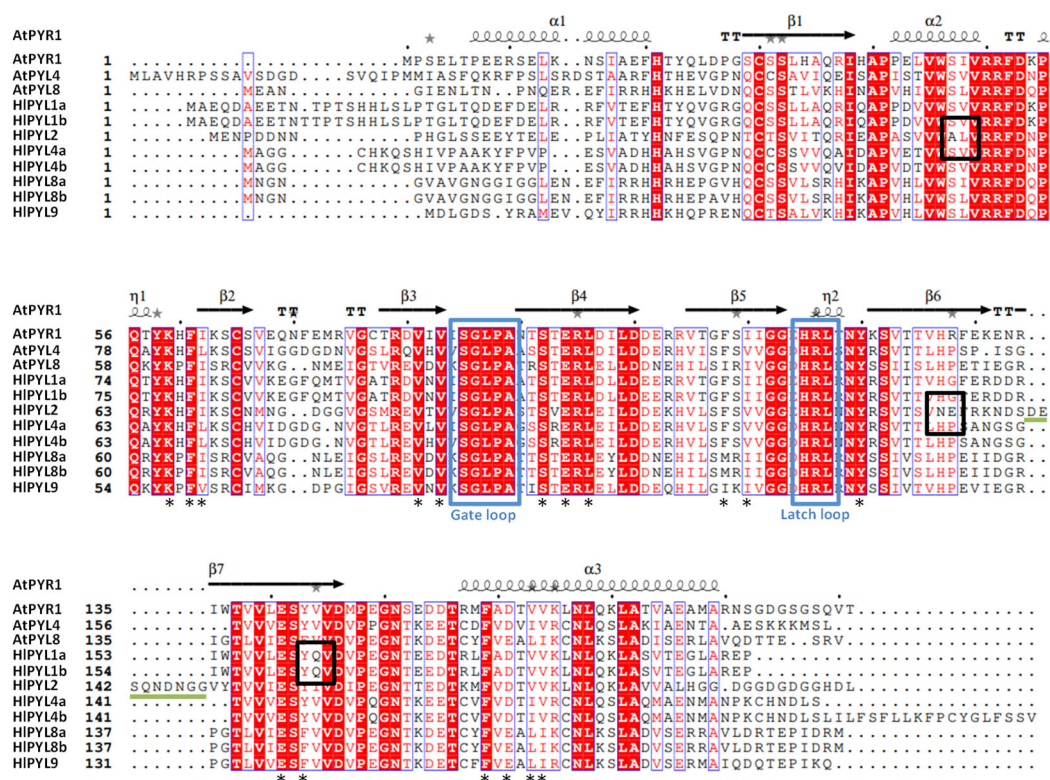


Figure 4. Amino acid sequence alignment of Arabidopsis and hop ABA receptors. Sequence and secondary structure alignment of ABA receptors are indicated. The secondary structure is shown according to the crystallographic structure of AtPYR1 (Protein DataBank Code 3k3k). The final visualization was generated using the ESPRIPT tool. Blue boxes indicate the position of the gate and latch loops. Black boxes indicate outstanding residue changes from consensus. Asterisks mark residues involved in interactions with ABA. Green line denote an extra loop found in *HIPYL2*.

This loop, in turn could modulates the ABA perception dynamics and/or the ternary complex ABA-PYL-PP2C formation. Furthermore, inside this loop we can see a putative phosphorylation target in S142. The function of this extra loop in HIPYL2 remains open to be characterized. Besides, in HIPYL2 we also detect a significant deviation from consensus sequence in the residue A54 and N132-E133. In the equivalent position of A54 is usually present a serine (S) in other PYLs, a putative phosphorylation target. Regarding N132-E133 (asparagine-glutamic acid) residues, the consensus at these positions is H-P (histidine-proline), and represents a significant change from a positive to a negative charge in this loop. Interestingly, N132-E133 residues are close to the latch loop and to the novel B6-B7 loop (Figure 4), in range to modify ABA binding and/or phosphatases interaction. On the other hand, we also detect a significant change in residues Q162/Q163 in HIPYL1a/b, respectively. The consensus at this position is the small hydrophobic residue valine (V) and HIPYL1a/b have a big polar glutamine (Q). This residue is also close to the latch loop and it is next to two key residues involved in ABA direct coordination: Y161/162 and E159/160 (Figure 4).

To further inspect the new features of HIPYL1 and 2, the protein 3D structure was obtained by homology modeling using the SwissModel in silico tool [70]. The models of HIPYL1b and HIPYL2 were obtained using as template the topology of SIPYL1 (PDB-ID 5mob) and AtPYL2 (PDB-ID 3kdh), respectively (Figures 5 and 6). Protein structure-estimated quality indicated that models were reliable (Supplemental Figures S3 and S4). In the topology analysis of HIPYL1b, residue **Q163** does not face the ABA interaction pocket (Figure 5A). Despite its close proximity to the latch loop and key residues involved in ABA binding, it is unlikely that Q163 disturbs or plays any significant role in hormone coordination. Furthermore, Q163 appears to be buried within the protein structure (Figure 5B), making it inaccessible for modulating homodimer or ternary complex formation. In contrast, the topology analysis of HIPYL2 reveals that residues A54, N132 and E133 are exposed on the protein surface (Figure 6A,B) and are therefore potentially accessible for mediating interactions with partners proteins. Although, the distance between these residues and the protein binding surface is not within the range necessary to influence interactions with other PYLs or phosphatases. Regarding the novel loop in HIPYL2, located between B6-B7 sheets, it is positioned on the side opposite to the gate of the ABA binding pocket and is unlikely to play a role in modulating ABA interactions or establishing the ternary complex. Nonetheless, this loop is exposed on the protein surface, and the phosphorylation-targeted residue S142 is accessible for modification by kinases (Figure 6A,B).

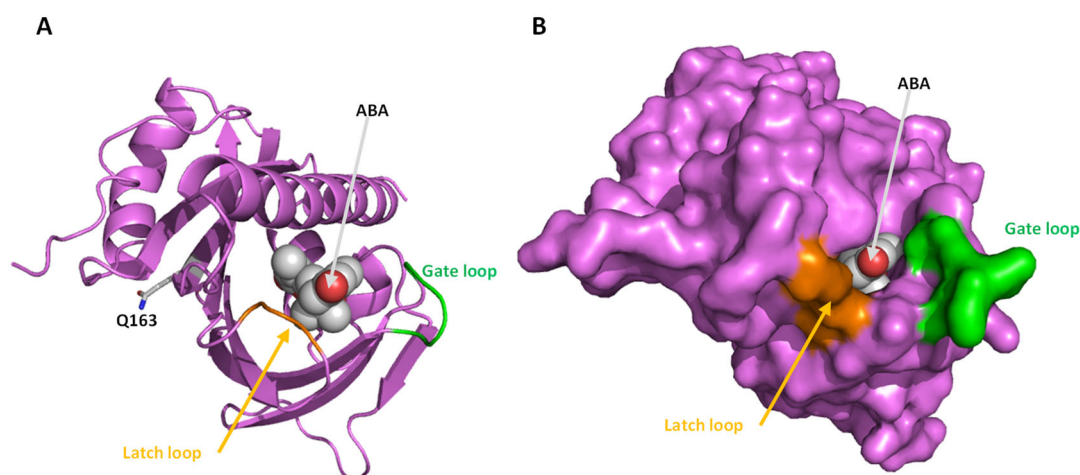


Figure 5. HIPYL1b protein 3D model. Topology was predicted by homology modeling in Swiss-Model using the PDB template 5mob. Model is showed by PyMOL as cartoons (A) and as protein surface (B). The model quality estimation by GMQE Global is 0.86 and QMEANDisCo Global: 0.85 ± 0.06 .

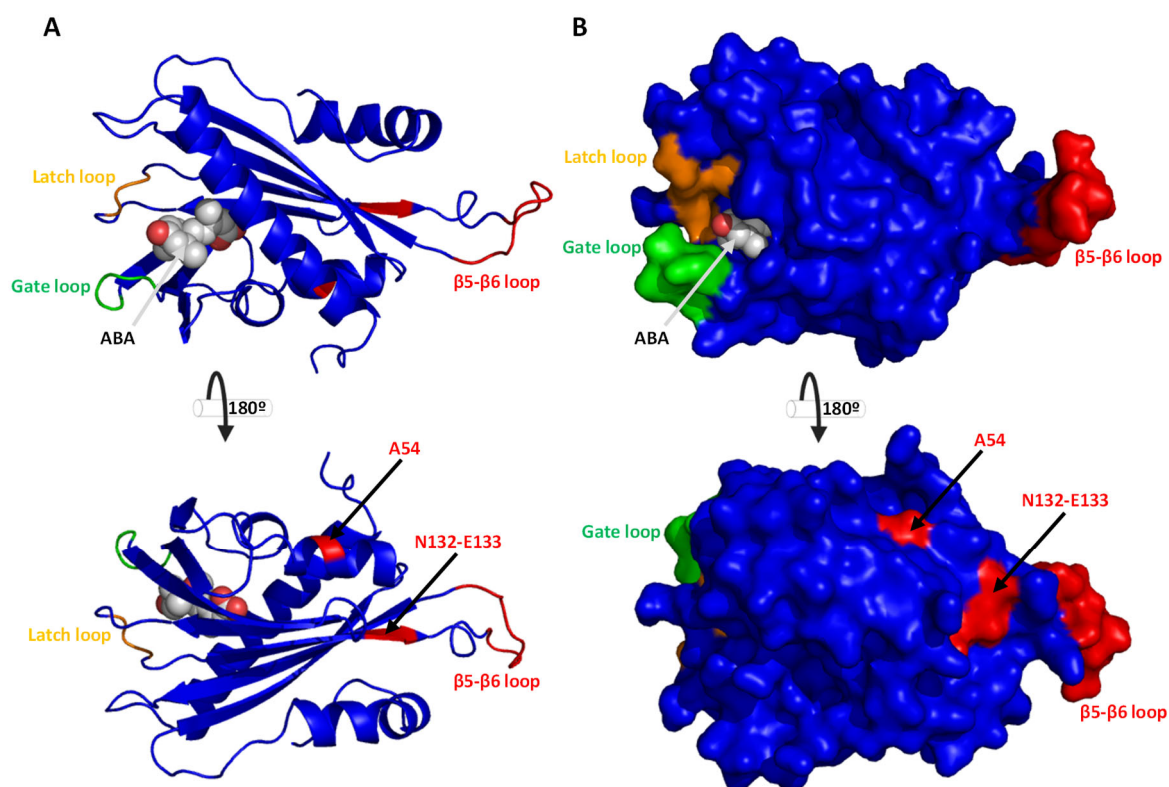


Figure 6. HIPYL2 protein 3D model. Topology was predicted by homology modeling in Swiss-Model using the PDB template 3kdh. Model is shown by PyMOL as cartoons (A) and as protein surface (B). The model quality estimation by GMQE Global is 0.81 and QMEANDisCo Global: 0.83 ± 0.05 .

2.4. ABA Effects in Plant Ex-Vitro Acclimatization and Transpiration

The acclimatization and rustication of whole plants derived from *in-vitro* culture is a critical step to ensure successful adaptation to the stressful *ex-vitro* environment. Usually, plant survival during this phase is often compromised by excessive water loss and premature senescence. The phytohormone ABA plays a central role in mediating plant responses to stress. However, after 21 days of transplantation into substrate under *ex-vitro* conditions, no significant difference in survival rate was observed between plants treated with 50 μM ABA (data not shown). Nevertheless, notable differences were detected in other phenotypic traits (Figure 7). Plants treated with 50 μM ABA showed significantly increased growth compared to mock-treated plants (mean plant height: 4.46 cm vs 2.73 cm respectively), a higher number of green leaves (17.07 vs 9.75) and fewer senescent leaves (2.92 vs 6.89), indicating improved physiological status and acclimatization under ABA.

In several plant species, ABA regulates leaf transpiration by modulating stomatal aperture [18,28]. However, this process remains uncharacterized in hop. To address this, a water loss assay was performed, revealing that treatment with 100 μM ABA significantly reduced leaf transpiration in hop (Figure 7A,B). Consistently, 10 μM ABA application also induces stomatal closure at both 4 and 24 hours post-treatment (Figure 7C,D), supporting a conserved role for ABA in promoting water retention through stomatal regulation.

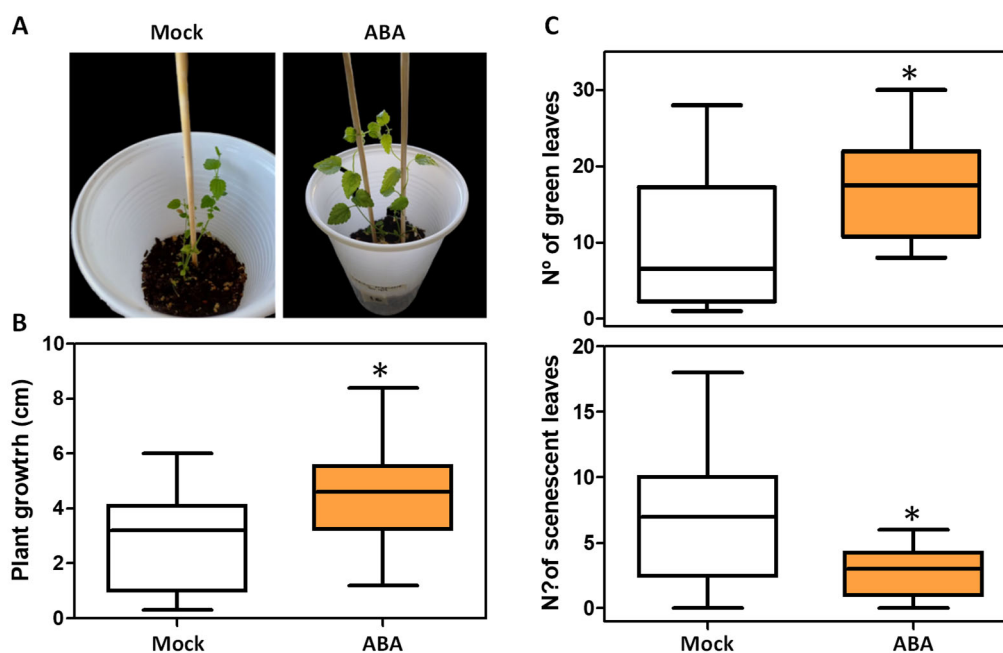


Figure 7. ABA treatment improves *in-vitro* acclimatization and rustication in *Humulus lupulus L. cv 'Mapuche'*. (A) A representative mock and 50 μM ABA sprayed plants; (B) plant growth quantification; (C) Number of green leaves (upper panel) and number of senescent leaves (lower panel). Phenotypes were evaluated after 21 days of *ex-vitro* growth. The asterisk indicates a significant difference respect to mock ($p \leq 0.05$).

3. Discussion

Abscisic acid (ABA) plays a pivotal role as a plant regulator, influencing various agronomical traits, including stress tolerance, seed maturation and germination, as well as shoots and root growth and development. Moreover, exogenous application of ABA has been shown to act as biostimulant, enhancing crop stress resilience [71]. Beyond plant systems, ABA can also be perceived by mammalian cells, where it has been proposed to improve several aspects of human health, including sleep disorders, depression, memory and pain [72].

ABA is a key hormone in the regulation of physiological responses to abiotic stress [16,17,44]. Central to ABA signaling is the PYRABACTIN RESISTANCE1-LIKE (PYL) gene family, which encodes the ABA receptors and initiates the signal transduction cascade. Identification and functional characterization of PYL receptors across species has highlighted their potential for improving stress tolerance traits such as drought and salinity resistance in crops [32,35,58,63,73]. These advances are particularly relevant in the context of global climate change, which demands new strategies for improving crop resilience [66,74–77].

In this study, we identified the ABA receptor gene family in *Humulus lupulus L.*, uncovering eight PYL genes distributed among the three classical phylogenetic clades: the dimeric PYL1-like subgroup (three members), and the monomeric PYL8-like and PYL4-like subgroups, with three and two members, respectively (Figure 2), accordingly to other reports in different crops [56,58,62,63,78]. Based on phylogenetic analysis, we propose standardized nomenclature for the eight HIPYLs based on their closest Arabidopsis orthologs (Table 1). Interestingly, the PYL4-like subfamily is underrepresented with only two members, a pattern previously reported only in *Citrus sinensis* [78], where this subfamily typically includes more genes. In contrast to *C. sinensis*, the expression of *HIPYL4a* and *HIPYL4b* is notably low across multiple tissues (Figure 3) suggesting a limited functional role. Instead, ABA perception in hop is likely mediated predominantly by members of the PYL1-like and PYL8-like subfamilies. In particular, *HIPYL1a*, *HIPYL1b*, *HIPYL8b*, and *HIPYL9* show strong expression in a range of tissues (adult leaves, shoots, roots, and cones) and developmental

stages (sprouting, vegetative, and flowering phases) (Figure 3). A similar pattern has been observed in *Phoenix dactylifera*, where PYL8-like receptors play a dominant role in ABA perception [62].

All eight HIPYL proteins contain a conserved PYR_PYL_RCAR domain, suggesting their potential functionality as ABA receptors (Supplemental Figure S2). This is further supported by the high degree of conservation observed in key residues and structural motifs, including the gate and latch loops that are critical for ABA binding (Figure 4). Interestingly, HIPYL2 possesses an additional loop near the latch region, which could, in principle, influence ABA perception dynamics and/or the formation of the ternary ABA-PYL-PP2C complex. However, topology analysis indicates that this extra loop is located on the opposite side of the ABA-binding gate (Figure 6) making a direct role in ABA binding or complex formation unlikely. Nonetheless, the presence of a putative phosphorylation site at residue S142 within this surface-exposed loop raises the possibility of a novel regulatory mechanism, which remains to be experimentally validated. In *Arabidopsis thaliana*, ABA receptor activity is modulated by multiple kinases, such as Target Of Rapamycin (TOR), Arabidopsis Early Flowering 1 (EL1)-like casein kinase (AEL), C-terminally Encoded Peptide Receptor 2 (CEPR2), and Cytosolic ABA Receptor Kinase 1 (CARK1), which fine-tune ABA signaling through phosphorylation [52].

In-vitro propagation of hop has been demonstrated as an effective technique to prevent pathogen transmission and ensure the clonal multiplication of female plants [9,10]. A critical step in this process is acclimatization or rustication, during which plantlets must adapt to the harsher *ex-vitro* environment, particularly by tolerating abiotic stresses [9,10]. ABA plays a central role in regulating drought tolerance [16–18], by promoting stomatal closure, enhancing antioxidant defenses, and stimulating the production of osmoprotectants. In this context, our results showed that ABA treatment in hop induced stomatal closure, significantly reduced leaf transpiration, and improved plant growth performance during *ex-vitro* acclimatization (Figures 7 and 8). These findings are consistent with previous reports demonstrating the positive effects of ABA application on plant acclimatization, such as in *Ulmus minor* [79]. Additionally, ABA may mitigate leaf stress and reduce senescence, thereby contributing to healthier plant development post-transplantation. Together, these observations emphasize the importance of considering post *in-vitro* culture treatments in securing successful plant adaptation to *ex-vitro* conditions.

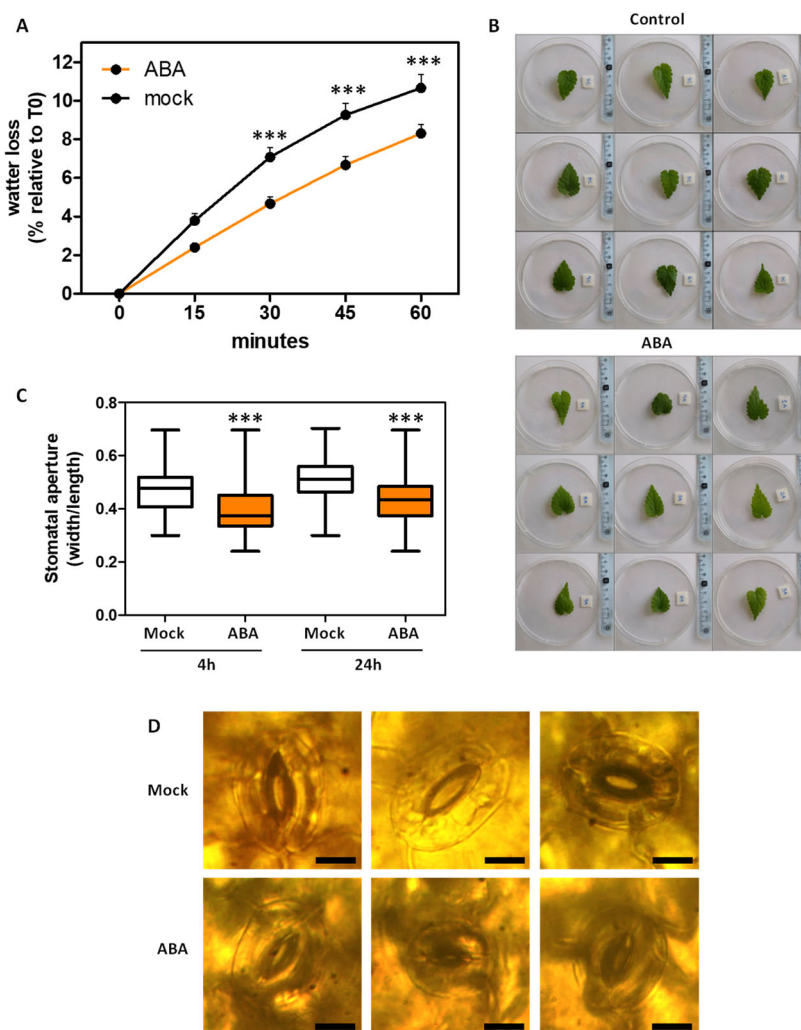


Figure 8. Transpiration and stomatal regulation by ABA in *Humulus lupulus L.* cv 'Mapuche'. (A) Loss of fresh weight of mock or 100 μ M ABA treated leaves. Line plot indicate mean \pm SE. (B) Photograph of representative excised leaves assayed in (A). (C) ABA-induced stomatal closure in hop leaves at 4h and 24h post treatment. Box plot mark interquartile ranges, mean (line), and max. and min. values (error bars) values (D) Photograph of representative stomatas measured at 24h post mock or 10 μ M ABA treatment; scale bars = 200 μ m. Student's t test were performed and asterisks indicate a significant difference respect to mock (** $p \leq 0.001$).

In conclusion, ABA perception in *Humulus lupulus L.* is likely mediated primarily by PYL1-like and PYL8-like receptors, leading to physiological responses such as stomatal closure and reduced leaf transpiration, which enhance *ex-vitro* acclimatization performance (Figure 9). This study lays a foundational framework for future functional analyses of *HlPYL* receptors and highlights the potential of utilizing ABA signaling to improve stress resilience in hop.

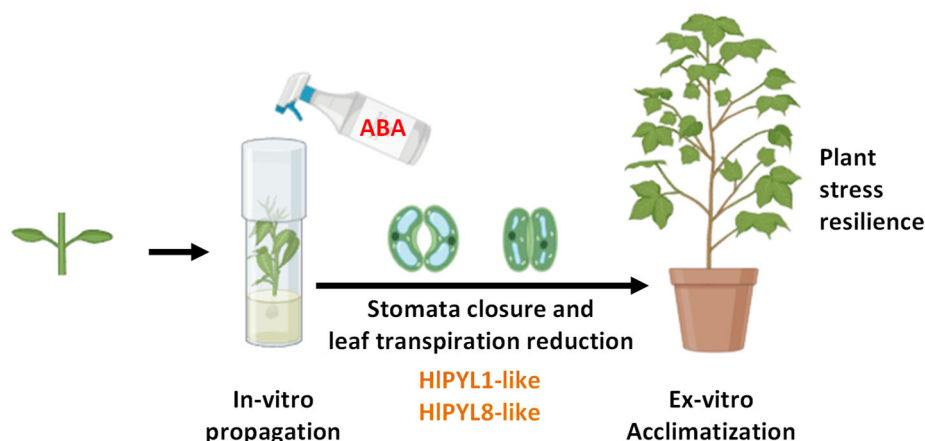


Figure 9. ABA enhance *ex-vitro* acclimatization performance in *Humulus lupulus L.* Hop acclimatization and rustication improvement after ABA treatment in terms of plant growth and stress symptoms. ABA in leaves could be perceived by receptors of dimeric PYL1-like and monomeric PYL8-like sub-families.

4. Materials and Methods

4.1. Genome-Wide Identification of PYL Genes in *Humulus lupulus L.*

The *Arabidopsis thaliana* PYL protein sequences were used as query to perform a BLASTP search against the local protein database of *Humulus lupulus L.* [64,65]: AtPYR1 (AT4G17870), AtPYL1 (AT5G46790), AtPYL2 (AT2G26040), AtPYL3 (AT1G73000), AtPYL4 (AT2G38310), AtPYL5 (AT5G05440), AtPYL6 (AT2G40330), AtPYL7 (AT4G01026), AtPYL8 (AT5G53160), AtPYL9 (AT1G01360), AtPYL10 (AT4G27920), AtPYL11 (AT5G45860), AtPYL12 (AT5G45870), AtPYL13 (AT4G18620). Eight unique proteins were identified and considered as candidate hop PYL proteins.

4.2. Phylogenetic and Gene Structure Analysis of HIPYLs

The chromosome physical location of the eight *HIPYL* was obtained from the HopBase genome DB [64,65]. A multiple sequence alignment of the eight identified hop proteins and 14 *Arabidopsis* PYLs was performed using ClustalW tool, followed by phylogenetic tree construction using the maximum-likelihood method (ML), using MEGA X (software version 10.2.6, [80] with a bootstrap value of 1000. The gene UTR–exon–intron structure of these eight *HIPYL* genes was obtained from the HopBase genome DB annotation files.

4.3. Analysis of ABA Receptor Expression in Hop Public Transcriptomic Data

Metadata for public RNA-Seq experiments (Illumina platform) assigned to *Humulus lupulus L.* were obtained from the Sequence Read Archive (SRA)-NCBI. These SRA metadata were automatically classified according to tissue, stage, cultivar, organism, and flower sex using the ontology-based system described in PlantaeViz [81]. The curated metadata is provided in Supplementary File S1, with a total of 61 runs for leaf, 25 runs for shoot system, two runs for cone, and 19 runs for root. These were used to evaluate expression of ABA receptors across different tissues. Runs were trimmed using fastp and aligned to the cv. “Cascade” hop genome using STAR (default parameters + -runMode alignReads --limitOutSJcollapsed 8000000 --limitIObufferSize 220000000). The gene models for the cv. “Cascade” hop genome, derived from maker and transdecoder, were obtained from HopBase [65]. Although gene ids with the “HUMLU_CAS” prefix were given to the combined transdecoder and maker gene set, a single combined gff was not provided by the database. Therefore, after individual transdecoder and maker gffs were obtained from the database, gene ids were renamed to the “HUMLU_CAS” structure based on a provided mapping file. A combined gff was generated with all gene models and their corrected gene ids, and the file is currently shared in

the PlantaeViz platform (<https://plantaeviz.tomsbiolab.com/hop/downloads/>). Count matrices were obtained using featureCounts (-t "exon" -C -g "featurecounts_id") using the combined annotation file and summarizing counts at the gene level by using a custom "featurecounts_id". Multimapping reads were not counted. Expression data was normalized to transcripts per kilobase of exon model per million mapped reads (TPM) values. To visualize the tissue-specific HIPYLs expression, a heat map was constructed using CLUSTVIS web tool [82].

4.4. Conserved Motifs Analysis, Protein Alignments and Homology Modeling of HIPYLs 3D Structure

The MOTIF search tool [83] was employed to identify the presence of the conserved PYR_PYL_RCAR domain within each HIPYL protein sequence, using both the Pfam and NCBI-CDD databases. This domain includes characteristic features such as the Polyketide cyclase/dehydrase and lipid transport domain, as well as the Bet_v1-like domain. Protein alignments between *Arabidopsis* (AtPYLs) and *hop* (HIPYLs) proteins were performed with the MegAlign7.0 software, from the DNASTAR Lasergene suite. Alignment graphics, along with the annotated secondary structure of AtPYR1 (Protein DataBank ID 3k3k), were generated using the Easy Sequencing in PostScript (ESPript) program [68]. To investigate protein 3D structure, **homology modeling** of HIPYL1b and HIPYL2 was carried out using the Swiss-Model interactive workspace [70]. Templates used for modeling were SIPYL1 (5mob, for HIPYL1b) and AtPYL2 (3kdh, for HIPYL2). Model quality was assessed using the QMEANDisCo global score function, along with the QMEANDisCo local scores (per residue) and several QMEAN z-scores, including QMEAN, C β , All Atom, Solvation, and Torsion scores. The QMEAN Z-score provides an estimate of the structural 'nativeness,' with higher values indicating more reliable models [84,85]. Based on these evaluations, the 3D models of both *HIPYL1b* and *HIPYL2* were considered reliable. Final 3D visualization and structural analysis were performed using Pymol (PyMOL Molecular Graphics System, Version 1.6 Schrödinger, LLC9).

4.5. Plant Material, ABA Treatment and Acclimatization to Ex-Vitro Conditions

Uninodal segments of *Humulus lupulus* L. cv. 'Mapuche' derived from *in-vitro* plants were cultured in 225 mL glass jars at 21±2°C under a long-day photoperiod (16:8 h light:dark) with a light intensity of 50 $\mu\text{mol}/\text{m}^2/\text{s}$ provided by white fluorescent lamps [10]. The culture medium consisted of half-strength Murashige and Skoog [86] basal medium (½ MS), supplemented with vitamins, macro- and micronutrients. The medium was solidified with 0.65% (w/v) agar (Sigma), supplemented with 3% (w/v) sucrose, and was adjusted to pH 5.8 prior to autoclaving 25 minutes at 121°C.

Following 21 days of *in-vitro* culture, fully developed seedlings were subjected to an acclimatization process. This process began 24 hours after a foliar application of 50 μM ABA solution or a mock treatment on both the adaxial and abaxial leaf surfaces, with 15 plants treated under each condition. Subsequently, the plants (N=30) were transferred to 220 ml pots filled with Growmix® substrate and covered with a film to maintain high humidity levels. The plants were incubated at room temperature under long day photoperiod in the growth room. During the first three weeks, the film was gradually opened, and fully removed at the end of this period. At this point, the following parameters were evaluated: plant survival, plant growth, and the number of green and senescent leaves. Then, surviving plants were transplanted into 0.5 liters pots and placed in an outdoor environment.

4.6. Leaf Transpiration and Stomatal Aperture Assays

Leaves from four-month-old *Humulus lupulus* L. cv 'Mapuche' plants were sprayed with 100 μM ABA 24 hours before sampling and then excised, together with untreated leaves (mock). The water loss kinetic analysis was subsequently measured. Data from nine leaves per treatment were plotted as the percentage of their initial fresh weight at each time point. Individual leaves were weighed every 15 minutes for three hours using an analytical balance. The experiment was repeated three times.

The stomatal aperture assay was conducted using whole-leaf images from four-month-old *Humulus lupulus* L. plants. To score ABA-induced stomatal closure, leaves were first incubated for 24 hours in stomatal opening buffer containing 10 mM KCl and 10 mM 2-(N-morpholino)-ethanesulfonic acid–KOH, pH 6.2, at 20°C. Subsequently, the leaves were incubated for 4 or 24 hours in fresh stomatal opening buffer, with or without the addition of 10 µM ABA [87]. Stomatal images were taken using Leica SFL 100 microscope with a Leica MC170 camera, and the aperture of 30 to 40 stomata per leaf (determined by width-to-length ratio) was measured using ImageJ 1.54g software in two independent experiments.

4.7. Statistical Analysis

Data were visualized in box plots. The statistical difference between mock and ABA treatments were calculated using t-test or one way ANOVA followed by Dunnet's test and p-value indicated with asterisks (*p ≤ 0.05; **p ≤ 0.01 and ***p ≤ 0.001).

Supplementary Materials: The following supporting information can be downloaded at the website of this paper posted on Preprints.org. Supplementary Figures S1–S4; Supplementary File S1.

Author Contributions: Conceptualization, L.D.S., P.B. and G.A.P.; methodology, L.D.S., F.Z., D.N.-P. and G.A.P.; software, D.N.-P.; formal analysis, L.D.S. and D.N.-P.; supervision, J.T.M., P.B. and G.A.P.; writing—original draft preparation, G.A.P.; writing—review and editing, L.D.S., D.N.-P., F.Z., J.T.M., P.B. and G.A.P. All authors have read and agreed to the published version of the manuscript.

Funding: This research received no external funding.

Conflicts of Interest: The authors declare no conflicts of interest.

References

1. Zanolì, P.; Zavatti, M. Pharmacognostic and pharmacological profile of *Humulus lupulus* L. *J. Ethnopharmacol.* **2008**, *116*, 383–396.
2. Uwe Koetter, M.B. Hops (*Humulus lupulus*): A review of its historic and medicinal uses. *HerbalGram* **2010**, *87*, 44–57.
3. Bertelli, D.; Brighenti, V.; Marchetti, L.; Reik, A.; Pellati, F. Nuclear magnetic resonance and high-performance liquid chromatography techniques for the characterization of bioactive compounds from *Humulus lupulus* L. (hop). *Anal. Bioanal. Chem.* **2018**, *410*, 3521–3531.
4. Neve, R. A. Hops. (Chapman and Hall, **1991**).
5. Roland, A.; Viel, C.; Reillon, F.; Delpech, S.; Boivin, P.; Schneider, R.; Dagan, L. First identification and quantification of glutathionylated and cysteinylated precursors of 3-mercaptohexan-1-ol and 4-methyl-4-mercaptopentan-2-one in hops (*Humulus lupulus*). *Flavour Fragr. J.* **2016**, *31*, 455–463.
6. Rettberg, N.; Biendl, M.; Garbe, L. A. Hop aroma and hoppy beer favor: Chemical backgrounds and analytical tools—A review. *J. Am. Soc. Brew. Chem.* **2018**, *76*, 1–20.
7. Lafontaine, S.; Scott Varnum, S.; Roland, A.; Delpech, S.; Dagan, L.; Vollmer D.; Kishimoto, T.; Shellhammer, T. Impact of harvest maturity on the aroma characteristics and chemistry of Cascade hops used for dry-hopping. *Food Chem.* **2019**, *278*, 228–239.
8. Faragó, J.; Psenáková, I.; Faragová, N. The use of biotechnology in hop (*Humulus lupulus* L.) improvement. *Nova Biotech.* **2009**, *9*(3), 279–293.
9. Agehara, S.; Acosta-Rangel, A.; Gallardo, M.; Vallad, G. Selection and Preparation of Planting Material for Successful Hop Production in Florida: HS1381, 9/2020. *EDIS: Gainesville, FL*, **2020**, 2020(5).
10. Di Sario L, Zubillaga MF, Moreno CFZ, Pizzio GA, Boeri PA. Micropropagation of Mapuche hop and evaluation of synthetic seed storage conditions. *PCTOC.* **2025**, *160*(2), 1-12.
11. Pospíšilová, J.; Synková, H.; Haisel, D.; Bařková, P. Effect of abscisic acid on photosynthetic parameters during ex-vitro transfer of micropropagated tobacco plantlets. *Biol. Plant.* **2009**, *53*, 11-20.

12. Dias, M. C.; Pinto, G.; Santos, C. Acclimatization of micropropagated plantlets induces an antioxidative burst: a case study with *Ulmus minor* Mill. *Photosynthetica*, **2011**, *49*, 259-266.
13. Osório, M. L.; Gonçalves, S.; Coelho, N.; Osório, J.; Romano, A. Morphological, physiological and oxidative stress markers during acclimatization and field transfer of micropropagated *Tuberaria major* plants. *PCTOC*. **2013**, *115*, 85-97.
14. Aguilar, M. L.; Espadas, F. L.; Coello, J.; Maust, B. E.; Trejo, C.; Robert, M. L.; Santamaria, J. M. The role of abscisic acid in controlling leaf water loss, survival and growth of micropropagated *Tagetes erecta* plants when transferred directly to the field. *J. Exp. Bot.* **2000**, *51*(352), 1861-1866.
15. Santamaria, J. M.; Davies, W. J.; Atkinson, C. J. Stomata of micropropagated *Delphinium* plants respond to ABA, CO₂, light and water potential, but fail to close fully. *J. Exp. Bot.* **1993**, *44*(1), 99-107.
16. Cutler, S.R.; Rodriguez, P.L.; Finkelstein, R.R.; Abrams, S.R. Abscisic Acid: Emergence of a Core Signaling Network. *Annu. Rev. Plant Biol.* **2010**, *61*, 651-679
17. Chen, K.; Li, G.; Bressan, R.A.; Song, C.; Zhu, J.; Zhao, Y. Abscisic acid dynamics, signaling, and functions in plants. *J. Integr. Plant Biol.* **2020**, *62*, 25-54.
18. Xu, X.; Liu, H.; Praat, M.; Pizzio, G.A.; Jiang, Z.; Driever, S.M.; Wang, R.; Van De Cotte, B.; Villers, S.L.Y.; Gevaert, K.; Leonhardt, N.; Nelissen, H.; Kinoshita, T.; Vanneste, S.; Rodriguez, P.L.; van Zanten, M.; Vu, L.D.; De Smet, I. Stomatal opening under high X temperatures is controlled by the OST1-regulated TOT3-AHA1 module. *Nature Plants* **2025**, *11*, 105-117.
19. Srecec, S.; Kvaternjak, I.; Kaucic, D.; Mariæ, V. Dynamics of Hop Growth and Accumulation of α -acids in Normal and Extreme Climatic Conditions. *Agric. Conspec. Sci.* **2004**, *69*, 59-62.
20. Mozny, M.; Tolasz, R.; Nekovar, J.; Sparks, T.; Trnka, M.; Zalud, Z. The impact of climate change on the yield and quality of Saaz hops in the Czech Republic. *Agric. For. Meteorol.* **2009**, *149*, 913-919.
21. Nakawuka, P.; Peters, T. R.; Kenny, S.; Walsh, D. Effect of deficit irrigation on yield quantity and quality, water productivity and economic returns of four cultivars of hops in the Yakima Valley Washington State. *Ind. Crops Prod.* **2017**, *98*, 82-92.
22. Donner, P.; Pokorný, J.; Ježek, J.; Krofta, K.; Patzak, J.; Pulkrábek, J. Influence of weather conditions, irrigation and plant age on yield and alpha-acids content of Czech hop (*Humulus lupulus* L.) cultivars. *Plant, Soil Environ.* **2020**, *66*, 41-46.
23. Chahtane, H.; Kim, W.; Lopez-Molina, L. Primary seed dormancy: a temporally multilayered riddle waiting to be unlocked. *J. Exp. Bot.* **2017**, *68*(4), 857-869.
24. Pan, W.; Liang, J.; Sui, J.; Li, J.; Liu, C.; Xin, Y.; Zhang, Y.; Wang, S.; Zhao, Y.; Zhang, J.; Yi, M.; Gazzarrini, S.; Wu, J. ABA and Bud Dormancy in Perennials: Current Knowledge and Future Perspective. *Genes (Basel)* **2021**, *12*(10), 1635.
25. De Smet, I.; Signora, L.; Beeckman, T.; Inzé, D.; Foyer, C.H.; Zhang, H. An abscisic acid-sensitive checkpoint in lateral root development of *Arabidopsis*. *Plant J.* **2003**, *33*, 543-555.
26. Jia, H.F.; Chai, Y.M.; Li, C.L.; Lu, D.; Luo, J.J.; Qin, L.; Shen, Y.Y. Abscisic Acid Plays an Important Role in the Regulation of Strawberry Fruit Ripening. *Plant Physiol.* **2011**, *157*, 188-199.
27. Gupta, K.; Wani, S.H.; Razzaq, A.; Skalicky, M.; Samantara, K.; Gupta, S.; Pandita, D.; Goel, S.; Grewal, S.; Hejnak, V.; Shiv, A.; El-Sabrou, A.M.; Elansary, H.O.; Alaklabi, A.; Brestic, M. Abscisic Acid: Role in Fruit Development and Ripening. *Front Plant Sci.* **2022**, *13*, 817-500.
28. Vishwakarma, K.; Upadhyay, N.; Kumar, N.; Yadav, G.; Singh, J.; Mishra, R.K.; Kumar, V.; Verma, R.; Upadhyay, R.G.; Pandey, M.; et al. Abscisic Acid Signaling and Abiotic Stress Tolerance in Plants: A Review on Current Knowledge and Future Prospects. *Front. Plant Sci.* **2017**, *8*, 161.
29. Tombesi, S.; Nardini, A.; Frioni, T.; Soccolini, M.; Zadra, C.; Farinelli, D.; Poni, S.; Palliotti, A. Stomatal closure is induced by hydraulic signals and maintained by ABA in drought-stressed grapevine. *Sci. Rep.* **2015**, *5*, 12449.
30. Falchi, R.; Petrusa, E.; Braidot, E.; Sivilotti, P.; Boscutti, F.; Vuerich, M.; Calligaro, C.; Filippi, A.; Herrera, J.C.; Sabbatini, P. Analysis of Non-Structural Carbohydrates and Xylem Anatomy of Leaf Petioles Offers New Insights in the Drought Response of Two Grapevine Cultivars. *IJMS* **2020**, *21*, 1457.

31. Saleh, B.; Alshehadah, E.; Slaman, H. Abscisic Acid (ABA) and Salicylic Acid (SA) Content in Relation to Transcriptional Patterns in Grapevine (*Vitis vinifera* L.) under Salt Stress. *J. Plant Biochem. Physiol.* **2020**, *8*, 245.
32. Lamers, J.; Zhang, Y.; van Zelm, E.; Leong, C.K.; Meyer, A.J.; de Zeeuw, T.; Verstappen, F.; Veen, M.; Deolu-Ajayi, A.O.; Gommers, C.M.M.; Testerink, C. Abscisic acid signaling gates salt-induced responses of plant roots. *Proc Natl Acad Sci U S A.* **2025**, *122*(6), e2406373122.
33. Alonso, R.; Berli, F.J.; Bottini, R.; Piccoli, P. Acclimation mechanisms elicited by sprayed abscisic acid, solar UV-B and water deficit in leaf tissues of field-grown grapevines. *Plant Physiol. and Biochem.* **2015**, *91*, 56-60.
34. Murcia, G.; Fontana, A.; Pontin, M.; Baraldi, R.; Bertazza, G.; Piccoli, P.N. ABA and GA3 regulate the synthesis of primary and secondary metabolites related to alleviation from biotic and abiotic stresses in grapevine. *Phytochem.* **2017**, *135*, 34-52
35. Pizzio, G.A.; Mayordomo, C.; Illescas-Miranda, J.; Coego, A.; Bono, M.; Sanchez-Olvera, M.; Martin-Vasquez, C.; Samantara, K.; Merilo, E.; Forment, J.; Estevez, J.C.; Nebauer, S.G.; Rodriguez, P.L. Basal ABA signaling balances transpiration and photosynthesis. *Physiol Plant.* **2024**, *176*(5), e14494.
36. Szekely, G.; Abraham, E.; Cseplo, A.; Rigó, G.; Zsigmond, L.; Csiszár, J.; Ayaydin, F.; Strizhov, N.; Jásik, J.; Schmelzer, E.; Koncz, C.; Szabados, L. Duplicated P5CS genes of Arabidopsis play distinct roles in stress regulation and developmental control of proline biosynthesis. *Plant J.* **2008**, *53*, 11-28.
37. Sengupta, S.; Mukherjee, S.; Basak, P.; Majumder, A.L. Significance of galactinol and raffinose family oligosaccharide synthesis in plants. *Front Plant Sci.* **2015**, *6*, 656.
38. Kirsch, F.; Klahn, S.; Hagemann, M. Salt-Regulated Accumulation of the Compatible Solutes Sucrose and Glucosylglycerol in Cyanobacteria and Its Biotechnological Potential. *Front Microbiol.* **2019**, *10*, 2139.
39. Nambara, E.; Marion-Poll, A. Abscisic acid biosynthesis and catabolism. *Annu. Rev. Plant Biol.* **2005**, *56*, 165–185.
40. Zhang, J.; Davies, W.J. Increased Synthesis of ABA in Partially Dehydrated Root Tips and ABA Transport from Roots to Leaves. *J. Exp. Bot.* **1987**, *38*, 2015–2023.
41. Zhang, J.; Davies, W.J. Changes in the concentration of ABA in xylem sap as a function of changing soil water status can account for changes in leaf conductance and growth. *Plant Cell Environ.* **1990**, *13*, 277–285.
42. Manzi, M.; Lado, J.; Rodrigo, M.J.; Zacarías, L.; Arbona, V.; Gómez-Cadenas, A. Root ABA Accumulation in Long-Term Water-Stressed Plants is Sustained by Hormone Transport from Aerial Organs. *Plant Cell Physiol.* **2015**, *56*, 2457–2466
43. McAdam, S.A.M.; Brodribb, T.J. Mesophyll Cells Are the Main Site of Abscisic Acid Biosynthesis in Water-Stressed Leaves. *Plant Physiol.* **2018**, *177*, 911–917.
44. Ruiz-Partida, R.; Rosario, S.; Lozano-Juste, J. An Update on Crop ABA Receptors. *Plants* **2021**, *10*, 1087.
45. Park, S.Y.; Fung, P.; Nishimura, N.; et. al. Abscisic acid inhibits type 2C protein phosphatases via the PYR/PYL family of START proteins. *Science* **2009**, *324*, 1068–1071.
46. Ma, Y.; Szostkiewicz, I.; Korte, A.; Moes, D.; Yang, Y.; Christmann A.; Grill, E. Regulators of PP2C phosphatase activity function as abscisic acid sensors. *Science* **2009**, *324*, 1064–1068.
47. Santiago, J.; Rodrigues, A.; Saez, A.; Rubio, S.; Antoni, R.; Dupeux, F.; Park, S.Y.; Márquez, J.A.; Cutler, S.R.; Rodriguez, P.L.; Modulation of drought resistance by the abscisic acid receptor PYL5 through inhibition of clade A PP2Cs. *The Plant Journal* **2009**, *60*, 575–588.
48. Umezawa, T.; Sugiyama, N.; Mizoguchi, M.; Hayashi, S.; Myouga, F.; Yamaguchi-Shinozaki, K.; Ishihama, Y.; Hirayama, T.; Shinozaki, K. Type 2C protein phosphatases directly regulate abscisic acid-activated protein kinases in Arabidopsis. *Proc. Natl. Acad. Sci. USA* **2009**, *106*, 17588–17593.
49. Vlad, F.; Rubio, S.; Rodrigues, A.; Sirichandra, C.; Belin, C.; Robert, N.; Leung, J.; Rodriguez, P.L.; Laurière, C.; Merlot, S. Protein Phosphatases 2C Regulate the Activation of the Snf1-Related Kinase OST1 by Abscisic Acid in Arabidopsis. *Plant Cell* **2009**, *21*, 3170–3184.
50. Zhu, J.K. Abiotic stress signaling and responses in plants. *Cell* **2016**, *167*, 313–324.
51. Coego, A.; Julian, J.; Lozano-Juste, J.; Pizzio, G.A.; Alrefaei, A.; Rodriguez, P. Ubiquitylation of ABA Receptors and Protein Phosphatase 2C Coreceptors to Modulate ABA Signaling and Stress Response. *IJMS* **2021**, *22*, 7103.

52. Pizzio, G.A. Abscisic Acid Machinery Is under Circadian Clock Regulation at Multiple Levels. *Stresses* **2022**, *2*, 65-78.
53. Pizzio, G.A.; Rodriguez, P.L. Dual regulation of SnRK2 signaling by Raf-like MAPKKs. *Mol. Plant* **2022**, *15*(8), 1260-1262.
54. Pizzio, G.A. Genome-Wide Identification of the PYL Gene Family in Chenopodium quinoa: From Genes to Protein 3D Structure Analysis. *Stresses* **2022**, *2*, 290-307.
55. Pizzio, G.A. Abscisic Acid Perception and Signaling in Chenopodium quinoa. *Stresses* **2023**, *3*(1), 22-32.
56. Sun, L.; Wang, Y.P.; Chen, P.; Ren, J.; Ji, K.; Li, Q.; Li, P.; Dai, S.J.; Leng, P. Transcriptional regulation of SIPYL, SIPP2C, and SlSnRK2 gene families encoding ABA signal core components during tomato fruit development and drought stress. *J. Exp. Bot.* **2011**, *15*, 5659-5669.
57. Boneh, U.; Biton, I.; Zheng, C.; Schwartz, A.; Ben-Ari, G. Characterization of potential ABA receptors in Vitis vinifera. *Plant Cell Rep.* **2012**, *31*, 311-321.
58. Bono, M.; Ferrer-Gallego, R.; Pou, A.; Rivera-Moreno, M.; Benavente, J.L.; Mayordomo, C.; Deis, L.; Carbonell-Bejerano, P.; Pizzio, G.A.; Navarro-Payá, D.; Matus, J.T.; Martinez-Zapater, J.M.; Albert, A.; Intrigliolo, D.S.; Rodriguez, P.L. Chemical activation of ABA signaling in grapevine through the iSB09 and AMF4 ABA receptor agonists enhances water use efficiency. *Physiol Plant.* **2024**, *176*(6), e14635.
59. Lei, P.; Wei, X.; Gao, R.; Huo, F.; Nie, X.; Tong, W.; Song, W. Genome-wide identification of PYL gene family in wheat: Evolution, expression and 3D structure analysis. *Genomics* **2021**, *113*, 854-866.
60. He, Y.; Hao, Q.; Li, W.Q.; Yan, C.Y.; Yan, N.E.; Yin, P. Identification and characterization of ABA receptors in Oryza sativa. *PLoS ONE* **2014**, *9*, e95246.
61. Di, F.F.; Jian, H.J.; Wang, T.Y.; Chen, X.P.; Ding, Y.R.; Du, H.; Lu, K.; Li, J.N.; Liu, L.Z. Genome-wide analysis of the PYL gene family and identification of PYL genes that respond to abiotic stress in Brassica napus. *Genes* **2018**, *9*, 156.
62. Garcia-Maquilon, I.; Coego, A.; Lozano-Juste, J.; Messerer, M.; de Ollas, C.; Julian, J.; Ruiz-Partida, R.; Pizzio, G.; Belda-Palazón, B.; Gomez-Cadenas, A.; et al. PYL8 ABA receptors of Phoenix dactylifera play a crucial role in response to abiotic stress and are stabilized by ABA. *J. Exp. Bot.* **2021**, *72*, 757-774.
63. Pizzio, G.A.; Mayordomo, C.; Lozano-Juste, J.; Garcia-Carpintero, V.; Vazquez-Vilar, M.; Nebauer, S.G.; Kaminski, K.P.; Ivanov, N.V.; Estevez, J.C.; Rivera-Moreno, M.; et al. PYL1- and PYL8-like ABA Receptors of Nicotiana benthamiana Play a Key Role in ABA Response in Seed and Vegetative Tissue. *Cells* **2022**, *11*, 795.
64. Hill ST.; Sudarsanam, R.; Henning, J.; Hendrix, D. HopBase: a unified resource for Humulus genomics. *Database* **2017**, bax009.
65. Padgitt-Cobb, L.K.; Kingan, S.B.; Wells, J.; Elser, J.; Kronmiller, B.; Moore, D.; Concepcion, G.; Peluso, P.; Rank, D.; Jaiswal, P.; Henning, J.; Hendrix, D.A. A draft phased assembly of the diploid Cascade hop (Humulus lupulus) genome. *Plant Genome* **2021**, *14*(1), e20072.
66. Gonzalez-Guzman, M.; Rodriguez, L.; Lorenzo-Orts, L.; Pons, C.; Sarrion-Perdigones, A.; Fernandez, M.A.; Peirats-Llobet, M.; Forment, J.; Moreno-Alvero, M.; Cutler, S.R.; et al. Tomato PYR/PYL/RCAR abscisic acid receptors show high expression in root, differential sensitivity to the abscisic acid agonist quinabactin, and the capability to enhance plant drought resistance. *J. Exp. Bot.* **2014**, *65*, 4451-4464.
67. Long, M.; Betrán, E.; Thornton, K.; Wang, W. The origin of new genes: Glimpses from the young and old. *Nat. Rev. Genet.* **2003**, *11*, 865-875.
68. Robert, X.; Gouet, P. Deciphering key features in protein structures with the new ENDscript server. *Nucleic Acids Res.* **2014**, *42*, W320-W324.
69. Moreno-Alvero, M.; Yunta, C.; Gonzalez-Guzman, M.; Lozano-Juste, J.; Benavente, J.L.; Arbona, V.; Menéndez, M.; MartinezRipoll, M.; Infantes, L.; Gomez-Cadenas, A.; et al. Structure of Ligand-Bound Intermediates of Crop ABA Receptors Highlights PP2C as Necessary ABA Co-receptor. *Mol. Plant* **2017**, *10*, 1250-1253.
70. Waterhouse, A.; Bertoni, M.; Bienert, S.; Studer, G.; Tauriello, G.; Gumienny, R.; Heer, F.T.; de Beer, T.A.P.; Rempfer, C.; Bordoli, L.; et al. SWISS-MODEL: Homology modelling of protein structures and complexes. *Nucleic Acids Res.* **2018**, *46*, W296-W303.

71. Di Sario, L.; Boeri, P.; Matus, J.T.; Pizzio, G.A. Plant Biostimulants to Enhance Abiotic Stress Resilience in Crops. *IJMS*, **2025**, *26*(3), 1129.
72. Pizzio, G.A. Potential Implications of the Phytohormone Abscisic Acid in Human Health Improvement at the Central Nervous. *System. Ann. Epidemiol. Public Health* **2022**, *5*, 1090.
73. Miao, C., Xiao, L., Hua, K., Zou, C., Zhao, Y., Bressan, R.A. et al. Mutations in a subfamily of abscisic acid receptor genes promote rice growth and productivity. *Proc. Natl. Acad. Sci. U. S. A* **2018**, *115*, 6058–6063.
74. Mosquna, A.; Peterson, F.C.; Park, S.Y.; Lozano-Juste, J.; Volkman, B.F.; Cutler, S.R. Potent and selective activation of abscisic acid receptors in vivo by mutational stabilization of their agonist-bound conformation. *Proc. Natl. Acad. Sci. USA* **2011**, *108*, 20838–20843.
75. Wang, Y.; Wu, Y.; Duan, C.; Chen, P.; Li, Q.; Dai, S.; Sun, L.; Ji, K.; Sun, Y.; Xu, W.; et al. The expression profiling of the CsPYL, CsPP2C and CsSnRK2 gene families during fruit development and drought stress in cucumber. *J. Plant Physiol.* **2012**, *169*, 1874–1882.
76. Pizzio, G.A.; Rodriguez, L.; Antoni, R.; Gonzalez-Guzman, M.; Yunta, C.; Merilo, E.; Kollist, H.; Albert, A.; Rodriguez, P.L. The PYL4 A194T mutant uncovers a key role of PYR1-LIKE4/PROTEIN PHOSPHATASE 2CA interaction for abscisic acid signaling and plant drought resistance. *Plant Physiol.* **2013**, *163*, 441–455.
77. Yang, Z.; Liu, J.; Poree, F.; Schaeufele, R.; Helmke, H.; Frackenpohl, J.; Lehr, S.; von Koskull-Döring, P.; Christmann, A.; Schnyder, H.; et al. Abscisic Acid Receptors and Coreceptors Modulate Plant Water Use Efficiency and Water Productivity. *Plant Physiol.* **2019**, *180*, 1066–1080.
78. Arbona, V.; Zandalinas, S.I.; Manzi, M.; González-Guzmán, M.; Rodríguez, P.L.; Gómez-Cadenas, A. Depletion of Abscisic Acid Levels in Roots of Flooded Carrizo Citrange (*Poncirus Trifoliata* L. Raf. × *Citrus Sinensis* L. Osb.) Plants Is a Stress-Specific Response Associated to the Differential Expression of PYR/PYL/RCAR Receptors. *Plant Mol. Biol.* **2017**, *93*, 623–640.
79. Dias, M. C.; Correia, C.; Moutinho-Pereira, J.; Oliveira, H.; Santos, C. Study of the effects of foliar application of ABA during acclimatization. *PCTOC* **2014**, *117*, 213–224.
80. Kumar, S.; Stecher, G.; Li, M.; Knyaz, C.; Tamura, K. MEGA X: Molecular Evolutionary Genetics Analysis across computing platforms. *Mol. Biol. Evol.* **2018**, *35*, 1547–1549.
81. Santiago, A.; Orduña, L.; Fernández, J.D.; Vidal, Á.; de Martín-Agirre, I.; Lisón, P.; Vidal, E.A.; Navarro-Payá, D.; Matus, J.T. The Plantae Visualization Platform: A comprehensive web-based tool for the integration, visualization, and analysis of omic data across plant and related species. *bioRxiv Bioinformatics*. **2024** <https://doi.org/10.1101/2024.12.19.629382>
82. Metsalu, T.; Vilo, J. Clustvis: A web tool for visualizing clustering of multivariate data using Principal Component Analysis and heatmap. *Nucleic Acids Res.* **2015**, *43*, W566–W570.
83. Motif Search. Available online: <https://www.genome.jp/tools/motif/> (accessed on October 1st 2023).
84. Benkert, P.; Biasini, M.; Schwede, T. Toward the estimation of the absolute quality of individual protein structure models. *Bioinformatics* **2011**, *27*, 343–350.
85. Studer, G.; Rempfer, C.; Waterhouse, A.M.; Gumienny, G.; Haas, J.; Schwede, T. QMEANDisCo—Distance constraints applied on model quality estimation. *Bioinformatics* **2020**, *36*, 1765–1771.
86. Murashige, T.; Skoog, F. A revised medium for rapid growth and bioassays with tobacco tissue cultures. *Physiol. Plant.* **1962**, *15*(3), 473–497.
87. Gonzalez-Guzman, M.; Pizzio, G.A.; Antoni, R.; Vera-Sirera, F.; Merilo, E.; Bassel, G.W.; et al. Arabidopsis PYR/PYL/RCAR receptors play a major role in quantitative regulation of stomatal aperture and transcriptional response to abscisic acid. *The Plant Cell.* **2012**, *24*(6), 2483–2496.

Disclaimer/Publisher's Note: The statements, opinions and data contained in all publications are solely those of the individual author(s) and contributor(s) and not of MDPI and/or the editor(s). MDPI and/or the editor(s) disclaim responsibility for any injury to people or property resulting from any ideas, methods, instructions or products referred to in the content.